Discharge of a Composite Metal Foam/Phase change material to Air Heat Exchanger for a Domestic Thermal Storage Unit

Pouyan Talebizadeh Sardari[1,*], Donald Giddings[1], David Grant[2], Mark Gillott[3], Gavin S Walker[2]

[1]Fluids and Thermal Engineering Research Group, Faculty of Engineering, University of Nottingham, University Park, Nottingham NG7 2RD, UK

[2]Advanced Materials Research Group, Faculty of Engineering, University of Nottingham, University Park, Nottingham NG7 2RD, UK

[3]Buildings, Energy and Environment Research Group, Faculty of Engineering, University of Nottingham, University Park, Nottingham NG7 2RD, UK

Abstract

This paper evaluates the discharging mechanism in a PCM (phase change material) to air heat exchanger for the purpose of space heating using a composite of copper foam and PCM. The composite system is modelled with both 2-D and 3-D computational fluid dynamics approach for different inlet air temperatures to consider the effect of room temperature using the thermal non-equilibrium model for the porous medium compared with the thermal equilibrium one. The results show the significant advantages of composite heat exchanger compared with a PCM only case. For the inlet air temperature of 22°C, the composite unit is solidified in 43% shorter time with 73% higher heat retrieval rate compared with that for the PCM only. After 10 hours, the temperature variation between the inlet and outlet of the air channels for latent heat storage heat exchanger system with the composite system is 41°C and 34°C for the inlet air temperatures of 0°C and 22°C, respectively, while it is 33°C and 29°C for the system with PCM only. This study show the possible usage of PCMs in the energy storage heaters by introducing metal foams which is not possible using PCM only alternatives.

[*] Corresponding author.

E-mail address: pouyan.talebizadehsardari@nottingham.ac.uk (P. Talebizadeh Sardari).

Keywords: PCM-air heat exchanger; Latent heat storage; Composite metal foam/PCM; Phase change material; Porous media; Discharging.

Nomenclature

A_m	The mushy zone constant	t_m	Melting/solidification time (s)
C	Inertial coefficient	T	Temperature (K)
C_p	PCM specific heat (J/kgK)	T_m	Melting point temperature (K)
d_l	Ligament diameter (m)	T_{ref}	Reference temperature (K)
g_i	Gravitational acceleration (m/s^2)	u_i	Velocity component (m/s)
h_{sf}	Local heat transfer coefficient inside the pores (W/m^{2}K)	$\vec{V}$	Velocity vector (m/s)
k_e, k_{eff}	Effective thermal conductivity (W/mK)	w	LHS rate density (W)
k_f	PCM thermal conductivity (W/mK)	**Greek symbols**	
k_s	Porous medium thermal conductivity (W/mK)	β	Thermal expansion coefficient (1/K)
K	Permeability (m^2)	ε	Porosity
L	Latent heat of fusion (J/kg)	λ	Liquid fraction
m	PCM Mass (kg)	μ	Dynamic viscosity (kg/ms)
P	Pressure (Pa)	ρ	Density (kg/m^3)
p	Rate of heat retrieval (W)	ρ_m	Density at melting point (kg/m^3)
Q	Heat retrieval capacity (J)	ΔH	Latent heat (J/kg)
q	Density of heat retrieval (J)	**Subscripts**	
Re_d	Local Reynolds number	ref	Reference

1. Introduction

Due to the higher consumption of energy in recent years and, as a result, higher production of pollutants and CO_2 emissions, improving energy efficiency and applying new methods to reduce energy consumption is essential. According to the UK energy consumption report, the domestic sector were responsible for 29 % of the total final energy consumption in 2015 which increased by 3.1% in 2016. Moreover, space and water heating account for 80% of the total energy consumption in buildings [1]. In 2016, the residential sector accounted for 18% of all CO_2 emissions which is 4.5% higher than 2015 [2].

Thermal energy storage (TES) in domestic heating applications can help balance the mismatch between energy supply and energy demand. TES employs to gain the excess energy that would otherwise be lost and permits load-shaving by charging the stored heat in off-peak hours. Among different kinds of TES systems including sensible, latent and chemical heat storage, there is growing interest in the usage of latent heat systems recently for heat storage due to having a high capacity of heat storage typically 5 to 14 times higher than sensible heat storage systems [3]. Furthermore, the characteristic of constant temperature during phase change is another feature of Latent heat systems which can also be employed to better control the output temperature. Latent heat storage (LHS) works by employing phase change materials (PCMs) and has been employed in various applications such as solar and geothermal systems, building heat exchangers, air conditioning systems, power plants and waste heat recovery [4, 5]. However, the rates of thermal diffusion within the bulk of PCM and also the thermal conductivity of PCMs are low which limit the use of LHS systems [6].

Different methods have been employed to overcome the limitation of PCM capability in the literature [7-22]. Composite metal foam/PCM has been developed recently as a substitute for PCM only due to heat transfer enhancement inside the PCM [23, 24]. Mesalhy et al. [25] showed significant effects of the presence of porous matrix within the PCM which enhances the rate of heat transfer and charging time. They recommended a foam with high porosity and high thermal conductivity due to reducing the convection effect by the use of the porous medium. Zhao et al. [26, 27] assessed the influences of porosity and pore density in a composite copper metal foam/PCM experimentally and numerically and showed significant increase of heat conduction rate by using a metal foam. The heat transfer increases 5-20 times in the PCM solid phase zone and 3-10 times in the mushy zone with metal foam compared with the PCM only in charging and discharging process. Liu et al. [28] studied numerically the melting of a composite metal foam/PCM shell and tube storage in 2-D and 3-D cases. They showed the small effect of pore size on the melting time. Zhang et al. [29] studied the melting process of a composite copper foam/paraffin LHS system in a 3-D rectangular enclosure heated from the left surface by electric heater. They showed that, compared with the paraffin only case, composite copper foam/paraffin has a higher heat transfer rate due to the presence of high conductivity copper foam. They presented that the mean charging powers of the paraffin only and composite PCM were estimated to be almost 4.19W and 4.28W at 3000s, respectively.

There are a few studies that work on the application of latent heat storage heat exchangers (LHSHE) for room heating and ventilation in the literature. Wang et al. [30] performed an experimental study on a high-temperature latent heat storage air heater in a room with the aim of transferring the electricity usage from the peak hours to off-peak hours. They used electrical elements to charge the PCM with a high latent heat and the melting point. The results show that by charging the system in 8 hours, the system can provide the suitable heat for room heating in the remaining 16 hours during the day. Dechesne et al. [31] studied an PCM air heat exchanger using in the ventilation system. In the system, for the heating purpose, heat gained from the PV modules is stored during the day and then is released to the room during the night. For cooling, coolness is stored during the night and release to the room during the day. They developed a semi-empirical equation for the outlet temperature of the air. The system can provide more than 50 W of cooling and heating powers by the PCM heat exchanger over five hours. Osterman et al. [32] prepared a PCM thermal energy storage suitable for both cooling and heating purposes to save energy. During summer, the system stores cold from the outdoor air at night to reduce the cooling load at the daytime and during winter, the system stores heat from the air heated by solar collectors for room heating. They showed that 142 kWh can be saved annually in the energy consumption of an office. Wang et al. [33] studied a PCM air heat exchanger with a zigzag plate geometry using different unequal mass PCMs with various melting points for industrial application. They validated their model with the experimental data using NaCl-$MgCl_2$ salt. The advantage of using different PCMs instead of only one PCM is that there is a time period within which the outlet temperature is almost equal to the initial temperature depending on the melting points of the employed PCMs and that there is improved uniformity of the system's output temperature using a proper design of PCM based heat storage systems.

As discussed in the literature review, there have been some studies in the literature on the application of latent heat storage heat exchangers using PCM only for domestic heating [30, 32, 34] and due to low thermal conductivity of PCMs, the number of publications has not significantly grown. Therefore, in this paper, an air-cooled LHSHE with composite metal foam and PCM is simulated numerically, and is compared with a PCM only system in the discharging process to study the uniformity of the system's output temperature and discharging time. The enthalpy-porosity method is employed for modelling the phase change while the optional thermal models of equilibrium and non-equilibrium are used for the porous medium. Effects of inlet air temperature on the performance of the system are studied in 2-D and 3-D cases. The effects of liquid fraction, temperature and velocity distributions, as well as the output temperature of the air to the room are examined. Different inlet temperatures are studied for the air as the input of the heater to simulate the real conditions inside the occupant place where different heat loads are required which has been rarely considered in the literature. It is noteworthy that for room heating, it is important to gain the desirable heat from the storage system during a limited time which is investigated comprehensively in this paper by introducing metal foams inside the PCM which cannot be achieved using PCM only alternative. This paper investigates the domestic thermal storage unit with the focus on the discharging time and output air temperature of the heat exchanger. The proposed system acts as a forced convention storage heater inside a room to provide the required heating load of the building taking the advantage of uniform output temperature.

2. Problem description

The PCM-air heat exchanger is studied numerically in 2-D and 3-D cases. The schematic of the 2-D domain is displayed in Fig. 1 for the PCM only (on the left) and the composite metal foam/PCM (on the right). In the system, composite PCM or PCM only is embedded in equal rectangular enclosures beside the air channel with adiabatic walls. There is a copper wall between the air channel and PCM container with a thickness of 1 mm which permits the heat to transfer from the PCM to the air. The dimensions of the system are displayed in the figure. The mass flow rate of air is considered to be 0.01 kg/s. For the composite case, the porosity of copper metal foam is 95% with a pore density of 50 PPI and pore size of almost 0.5 mm. It should be noted that the volume of the system for both composite PCM and PCM only case are equal.

Note that different points at the middle of PCM shell with the distance of 10 cm with each other are considered in both composite PCM and PCM only cases to better compare the results of temperature at different location. The points are displayed in Fig. 1 by green cross sign in the PCM only case to better understanding their locations.

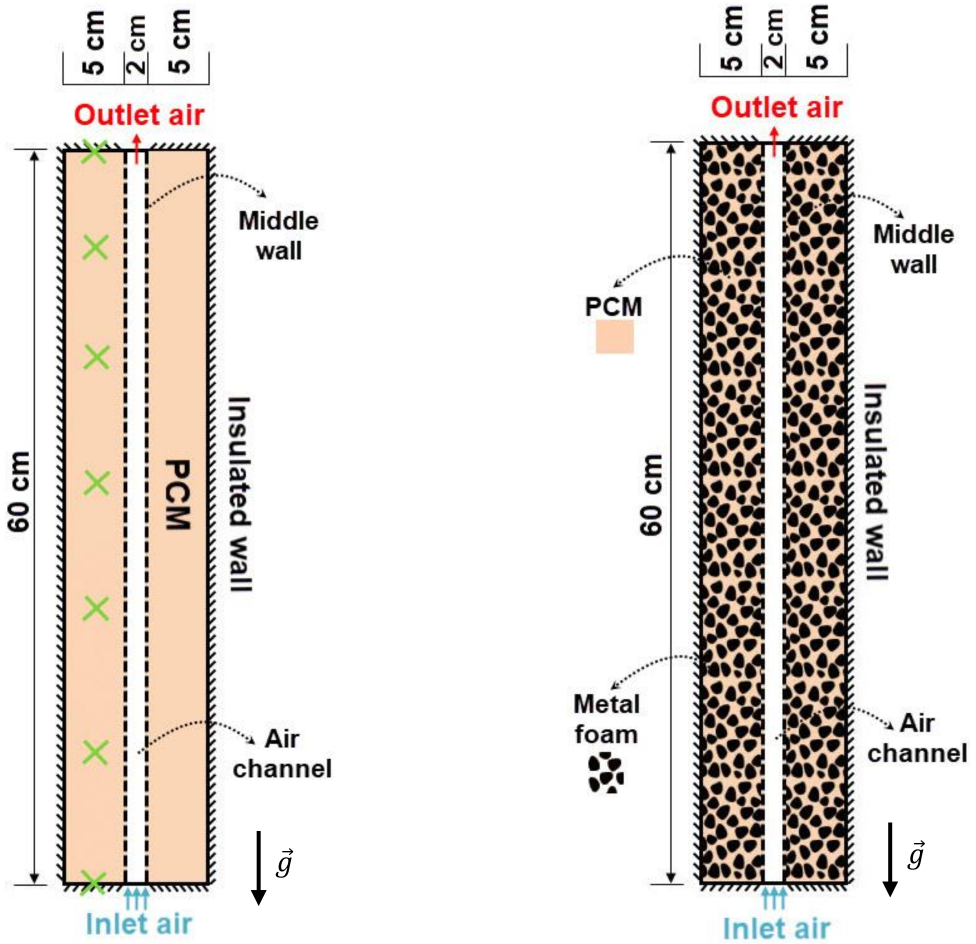

Fig. 1. The schematic of the 2-D geometry for the PCM-air heat exchanger with a) a PCM only and b) a composite metal foam/PCM

The schematic of the 3-D computational domain and the way of passing air inside the system are shown in Figs. 2-a and 2-b, respectively. The difference between the 2-D and 3-D cases is the insulated walls at the left and right sides of the system. It is noteworthy that regarding the typical dimensions of radiator units, the length and height of the proposed system are chosen as 1 m and 60 cm, respectively. Moreover, the width of the PCM container and air channel are 10 cm and 2 cm, respectively.

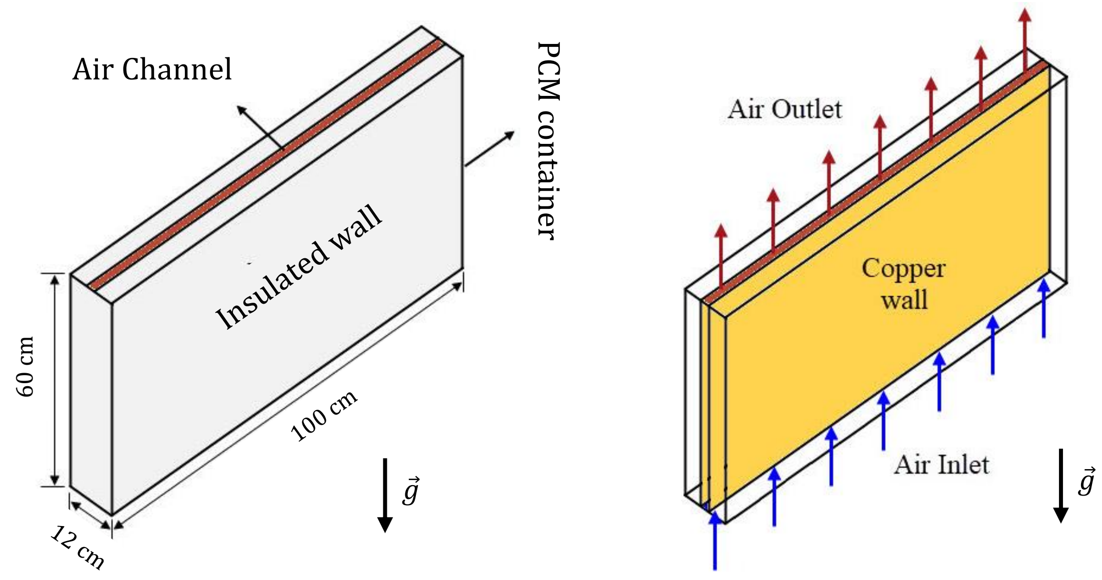

a) b)

Fig. 2. The schematic of the 3-D geometry for the PCM-air heat exchanger: a) dimensions of the system and b) the way of air entrance and exit

3. PCM material

An organic PCM RT-82 (RUBITHERM) is used in the simulations, the thermophysical properties of RT-82 as well as the thermophysical properties and specifications of copper foam are listed in Table 1. Note that according to the properties of RT-82, the density is phase-dependent and in the liquid state, due to thermal expansion of the PCM, the density varies with temperature. Therefore, a UDF is provided to calculate the density in different phases according to the PCM liquid fraction and temperature. It is considered as constant 880 kg/m^3 in the solid state, linear variation in the mushy zone between 880 and 770 kg/m^3, and then, at the liquid state, density is varied according to the Boussinesq approximation given as:

$$\rho = \frac{\rho_l}{\beta(T - T_l) + 1} \tag{27}$$

where β is the thermal expansion coefficient, T is the fluid temperature, T_l is the liquidus temperature, ρ is the density and ρ_l is the PCM density at liquidus temperature.

The reason for selecting RT-82 is domestic heating application. As an air heater for domestic space heating, the range of output temperature should be between 30-50 ºC. Since by using this material with the melting point of 82 ºC, an acceptable output temperature is provided, therefore this material is used as the PCM in this study.. There is the added advantage that at 82°C, the PCM in the insulated cavity will have a low temperature gradient compared to either hotter PCM materials (e.g. salt PCM) or the traditional sensible heat storage blocks which are generally in the order of 100s of °C.

Table 1

RT 82 properties [35]

Property	RT 82
T_s/T_f (°C)	77/82
L (kJ/kg)	170
C_p (kJ/kgK)	2
ρ (kg/m^3)	880 (solid) – 770 (liquid)
k_f (W/mK)	0.2
μ (Pa s)	0.03499
β (1/K)	0.001
Property	Copper
Density	8960 (kg/m^3)
Thermal conductivity	400 (W/m.K)
Specific heat	0.385 (kJ/kg.K)
Porosity	95%
Pore density	50 PPI

Note that the entire system is initially at the temperature of 85 °C which is 3 °C higher than the liquidus temperature of the PCM.

4. Mathematical modelling

Standard numerical methods are applied as outlined in the following, with the addition of the formulae from literature for the phase change representation which are developed into a user defined function. Enthalpy-porosity model is employed to model the effect of phase change in the LHSHE systems. In the presence of a porous medium based on the viscous and inertial losses, an addition pressure drop is considered in the momentum equation [36]. For simulating heat transfer in the porous media, two thermal models are used i.e. the equilibrium and non-equilibrium. In the equilibrium model, the temperature of liquid PCM and the porous medium are the same, but in the non-equilibrium one, the porous medium and PCM are not considered to be in thermal equilibrium which is more accurate, and is employed in this study considering the assumptions below [28, 37, 38]:

1. Incompressible Newtonian fluid for the liquid PCM
2. Open-cell, homogeneous and isotropic metal foam
3. Negligible Viscous dissipation
4. Constant thermo-physical properties except the density for the PCM

Therefore, the set of governing equations for the Brinkman–Forchheimer-extended Darcy model are given as [23]:

Continuity:

$$\frac{\partial \rho}{\partial t} + \nabla . \rho \vec{V} = 0 \tag{1}$$

Momentum:

$$\frac{\rho_f}{\varepsilon}\frac{\partial u_i}{\partial t} + \frac{\rho_f}{\varepsilon^2}\left(\vec{V}.\nabla u_i\right) = -\frac{\partial P}{\partial x_i} + \frac{\mu_f}{\varepsilon}\left(\nabla^2 u_i\right) - A_m \frac{(1-\lambda)^2}{\lambda^3 + 0.001} u_i - \left(\frac{\mu_f}{K} + \frac{\rho_f C|u_i|}{\sqrt{K}}\right) u_i - \rho_f g_i \beta \varepsilon \left(T - T_{ref}\right) \tag{2}$$

A_m is the mushy zone constant considered equal to 10^5 [39]. K and C can be fined in Ref. [36]. The energy equation for equilibrium and non-equilibrium thermal models are given as follows [28]:

Equilibrium thermal model:

$$\varepsilon\rho_f\left(C_f + L\frac{d\lambda}{dT_f}\right)\frac{\partial T_f}{\partial t} + \rho_f C_f(\vec{V}.\nabla T_f) = k_e\nabla^2 T_f \tag{3}$$

Non-equilibrium thermal model:

For the PCM:

$$\varepsilon\rho_f\left(C_f + L\frac{d\lambda}{dT_f}\right)\frac{\partial T_f}{\partial t} + \rho_f C_f(\vec{V}.\nabla T_f) = k_{fe}\nabla^2 T_f - h_{sf}A_{sf}(T_f - T_s) \tag{4}$$

For the porous medium:

$$(1-\varepsilon)\rho_s C_s\left(\frac{\partial T_s}{\partial t}\right) = k_{se}\nabla^2 T_s - h_{sf}A_{sf}(T_s - T_f) \tag{5}$$

where for the equilibrium model, k_e is the volume average of k_f and k_s. In the non-equilibrium one, the effective thermal conductivity is defined as follows [28]:

$$k_{eff} = \frac{1}{\sqrt{2}(R_A + R_B + R_C + R_D)} \tag{6}$$

where

$$R_A = \frac{4\sigma}{(2e^2 + \pi\sigma(1-e))k_s + (4 - 2e^2 - \pi\sigma(1-e))k_f} \tag{7}$$

$$R_B = \frac{(e-2\sigma)^2}{(e-2\sigma)e^2 k_s + (2e - 4\sigma - (e-2\sigma)e^2)k_f} \tag{8}$$

$$R_C = \frac{\sqrt{2} - 2e}{\sqrt{2}\pi\sigma^2 k_s + (2 - \sqrt{2}\pi\sigma^2)k_f} \tag{9}$$

$$R_D = \frac{2e}{e^2 k_s + (4 - e^2)k_f} \tag{10}$$

where $e = 0.16$ and

$$\sigma = \sqrt{\frac{\sqrt{2}(2 - \left(\frac{3\sqrt{2}}{4}\right)e^3 - 2\varepsilon)}{\pi(3 - 2\sqrt{2}e - e)}} \tag{11}$$

To calculate k_{fe} from Eq. (10), k_{se} should be considered zero in Eqs. (11-14) substituted to Eq. (10). On the other hand, to calculate k_{se}, k_{fe} should be considered zero in Eq. (10-14). Therefore, it can be expressed as follows:

$$k_{fe} = k_{eff}|k_{s=0} \tag{12}$$

$$k_{se} = k_{eff}\big|k_{f=0} \tag{13}$$

To determine the local heat transfer coefficient between the porous medium and PCM, the porous structure is usually considered as cylinders and the laminar flow of liquid PCM in porous structure is considered similar to the flow around a cylinder. Therefore, in Eqs. (8-9), the interstitial heat transfer coefficient is calculated as [40, 41]:

$$h_{sf} = 0.76Re_d^{0.4}Pr^{0.37}k_{pcm}/d_l \tag{14}$$

where

$$Re_d = \rho_{pcm}\sqrt{u^2 + v^2}d_l/(\varepsilon\mu_{pcm}) \tag{15}$$

and d_l can be find in Ref. [36].

In the porous medium, in addition to the temperature of the PCM, the fluid velocity depends on the characteristics of the metal foam. During the solidification process, when the PCM starts to solidify and the heat is transferred from the PCM to the air, the velocity increases due to the start of natural convection effect; however, due to flow resistance by the porous structure, the fluid movement is supressed and the velocity decreases. In our case, the maximum velocity is less than 0.01 mm/s and as a result the calculated Re_d by Eq. (19) is small. The general form of h_{sf} depends on the Reynolds number; however, due to the small magnitude of the Reynolds number, Eq. (18) is employed in this study. The general form can be found in Ref. [41]. A_{sf} is the specific surface area of the porous medium given as [41]:

$$A_{sf} = \frac{3\pi d_l (1 - e^{-(1-\varepsilon)/0.04})}{0.59 {d_p}^2} \tag{16}$$

In the energy equation (Eq. (8)), λ is the liquid fraction which is defined as [42]:

$$\lambda = \frac{\Delta H}{L} = \left\{ \begin{array}{cc} 0 & if \;\; T < T_{Solidus} \\ 1 & if \;\; T > T_{Liquidus} \\ \dfrac{T - T_{Solidus}}{T_{Liquidus} - T_{Solidus}} & if \;\; T_{Solidus} < T < T_{Liquidus} \end{array} \right\} \tag{17}$$

where ΔH is the fractional latent heat of the PCM that may vary between zero for solid and L (latent heat of fusion) for liquid.

It should be noted that the porosity is considered 1 for the PCM only case in the above equations which causes the cell diameter of zero results in the elimination of porous media source terms in the momentum equations.

Different parameters including the rate of heat retrieval, heat retrieval density and heat retrieval rate density are defined to assess the performance of the system. The rate of heat retrieval is defined as the ratio of the heat storage capacity to the solidification time [43]:

$$p = \frac{Q}{t_m} = \frac{m_{por} \int c_{p,por} dT + m_{pcm} \left(\int_{solid} c_{p,pcm} dT + L_f + \int_{liquid} c_{p,pcm} dT \right)}{t_m} \approx \frac{m_{pcm} L_f}{t_m} \tag{20}$$

The heat retrieval density is the heat retrieval rate over the summation of PCM and metal foam masses [43]:

$$q = \frac{Q}{m} = \frac{m_{por} \int c_{p,por} dT + m_{pcm} \left(\int_{solid} c_{p,pcm} dT + L_f + \int_{liquid} c_{p,pcm} dT \right)}{m_{por} + m_{pcm}} \approx \frac{m_{pcm} L_f}{m_{por} + m_{pcm}} \tag{21}$$

Heat retrieval rate density is also used to consider all parameters of mass, melting/solidification time and heat retrieval capacity together, as the ratio of heat storage/retrieval rate to the mass of the composite material defined as [43]:

$$w = \frac{Q}{t_m m} = \frac{m_{por}\int c_{p,por}dT + m_{pcm}\left(\int_{solid} c_{p,pcm}dT + L_f + \int_{liquid} c_{p,pcm}dT\right)}{t_m(m_{por}+m_{pcm})} \approx \frac{m_{pcm}L_f}{t_m(m_{por}+m_{pcm})} \tag{22}$$

Note that for the PCM only case, in Eqs. 25-26, m_{por} is zero.

5. Numerical procedure

ANSYS-FLUENT software is employed to solve the governing equations using double precision solver with SIMPLE algorithm due to incompressible flow. A user-defined function (UDF) is employed for calculating both the interfacial heat transfer coefficient between the liquid PCM and metal foam and the density variation of the PCM. PRESTO pressure interpolation scheme is used due to buoyancy, while the quadratic upwind discretisation, QUICK, scheme is employed for the momentum and energy equations, both for enhancing accuracy of the numerical method. The mesh independency analysis for both 2D and 3D cases are performed precisely in this study which are presented in Appendix-(A).

Furthermore, the time step size is considered 0.5s with the maximum number of 200 iterations for each time step. The results are not varied by reducing the size of time step. The same procedure is performed for the LHSHE with the PCM only and the value of time step is considered 0.25s with the same mesh and maximum number of time steps for PCM only case. Note that for the selected size of the mesh and time step, and for the inlet air temperature of 22 ^{o}C, for the equilibrium model, the computational time is almost 2.5 days for the 3D and 1 day for the 2D geometry using Fluent in parallel mode with 4 cores after 65,000 s (18 hours) of simulation time.

6. Validation

In this study, a comprehensive validation process is performed for all the cases of PCM only as well as equilibrium and non-equilibrium thermal models of porous-PCM. All the comparisons are made with both numerical and experimental studies form the literature.

For the composite case, the 2D numerical and the experimental results of Zhao et al. [26, 27] as well as 2D numerical study of Liu et al [28] are used for validation. The studied geometry was a rectangular heat storage unit with the dimensions of 200 mm × 50 mm with 1.6 kW/m^2 heat flux from the bottom using RT-58 for the PCM and copper foam with the porosity of 95%. To have a more accurate results, heat loss into the surrounding was also considered for the other walls in the numerical model. The temperature at the height of 8mm is presented in comparison with Zhao et al [26, 27] and in Fig. 3 and an excellent agreement can be found between the non-equilibrium thermal model and the numerical and experimental results of Zhao et al. and numerical results of Liu et al. The results of the equilibrium thermal model is also in good agreement with the equilibrium modelling of Liu et al [28]. Furthermore, as mentioned in [28], the numerical results of Zhao et al. have a small variation with the experimental results due to considering a constant melting temperature. However, in this study and the study of Liu et al. [28], different liquidus and solidus temperatures are considered for the simulations. A maximum deviation of ±4.2°C achieved between the present results and experimental data of Zhao et al. It should be noted that it is difficult to justify the accuracy of this discrepancy according to the figure since the data from the experiment is taken from the electronic copy of Zhou et al and will suffer perhaps up to 2°C positioning error compared to the present data. Therefore we put in a statement offering the qualification of results that they may deviate from physical results according to the uncertainty of our method by up to 5°C, but that the trends observed will be self-consistent, as observed in Fig. 3

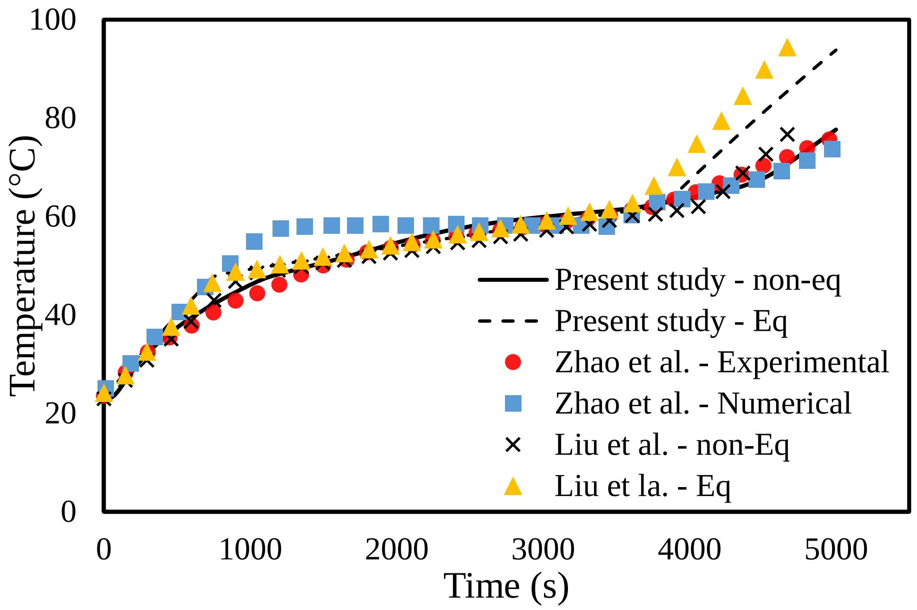

Fig. 3. The validation results of composite PCM compare with different numerical and experimental works [27, 28]

For the code validation in a solidification problem with and without considering the foam, the numerical results of Esapour et al. [15] are employed for comparison. They modelled a porous-PCM LHS system numerically in a triple-tube heat exchanger using Rt-35 as the phase change material. Fig. 4 illustrates the variation of liquid fraction for the current study compared with the results of Esapour et al. [15] showing an excellent agreement during the solidification process. This work relied for validation on the experiments of Zhou et al. in terms of determining the reliability of the numerical method for the phase change, and then they go on to simulate solidification using the same validated methodology. In the same way, we validate against the melting experiment of Zhou et al. and use the proven application of the methodology in our simulations for simulation of solidification process since the phase change algorithm is similar in melting and solidification.

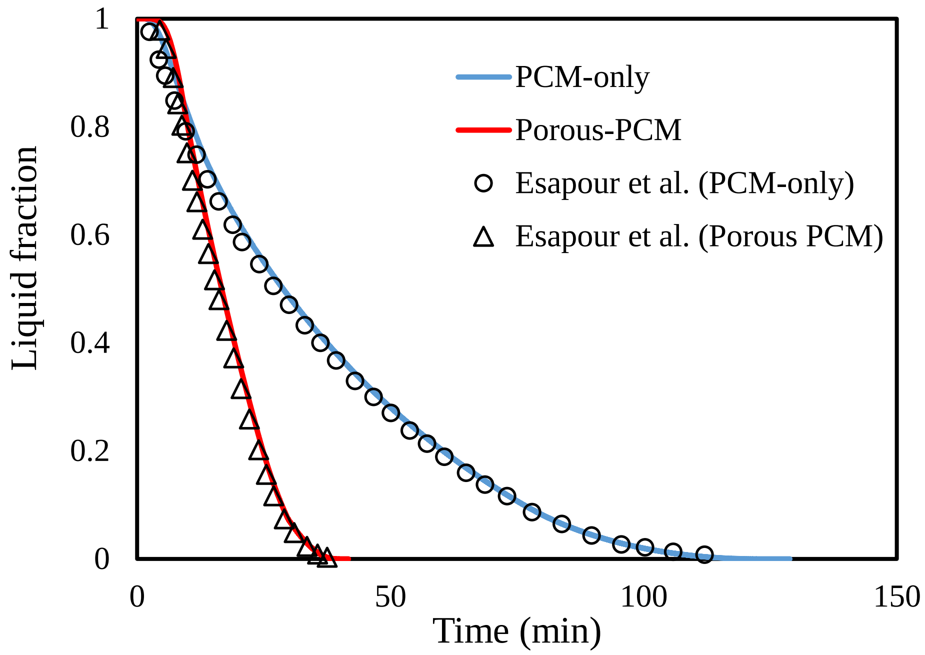

Fig. 4. The validation results for the solidification process in a triple-tube porous-PCM LHS unit in compare with Ref. [15]

7. Results and discussion

In the solidification process of the proposed heat exchanger, cold air is passed through the middle of the system from bottom to the top, the air gains heat from the PCM in order to reach the desired temperature at the outlet. Three inlet temperatures of 0°C, 10°C and 22°C are examined to simulate the heat exchanger at three different periods of time as follows:

1- The initial time when the system starts heating a very cold room (cold start).
2- The middle stage when the room temperature rises to higher temperatures at 10°C
3- The final stage when the room reaches the thermal comfort temperature

At the cold start, the heat exchanger should provide more heat to increase the room temperature to the thermal comfort condition quickly. Furthermore, at the final stage, the heat exchanger should provide almost constant heat to keep the room temperature almost constant to balance against steady heat loss from a room. It is noteworthy that the heat exchanger works mostly in the third state when inlet air temperature is 22°C, equal to the thermal comfort temperature.

This selected target temperature is within the range according to ASHRAE standard, for thermal comfort, 19.5°C and 27.8°C [44, 45].

7.1. 2-D simulation of a composite PCM-air heat exchanger compared with the case of PCM only

In this section, first, the results for the inlet air temperature of 22°C are discussed for the system with the composite PCM compared with the PCM only and then the effects of different inlet air temperatures are investigated.

Fig. 5 displays the contours of temperature distribution for the PCM-air heat exchanger for both the composite PCM and the PCM only systems at different times. As shown in the air channel, the air enters the channel at a temperature of 22°C, gaining heat from the PCM as it passes through the channel. The PCM releases heat to the air and then when its temperature drops down to the liquidus temperature, solidification starts. Since the air enters from the bottom of the system, the bottom area of the system is colder than the top area. Therefore the solidification starts from the bottom. In other words, the near region of the air channel solidifies by conduction heat transfer while the heat is transferred by both conduction and natural convection in the PCM domain. In the composite LHSHE, the heat transfer rate is considerably enhanced due to the presence of metal foam by conduction in the main body of PCM and the heat is transferred faster [27]. Note that the effect of natural convection is very low due to high flow resistance because of the tortuosity of the porous medium. In the LHSHE with the PCM only, natural convection is dominant for heat transfer mechanism after the initial minutes when the heat is transferred by only conduction. The results show that the velocity magnitude of liquid PCM for the composite case is almost zero; however, in the PCM only, the PCM starts moving at the beginning and the velocity reaches almost 1.4 mm/s and then reduces due to the solidification process. As shown, the effect of natural convection in the PCM only system is much smaller than the effect of the porous medium in the composite system regarding heat transfer enhancement. After 18 hours, while the temperature of the composite case is between 50°C and 56°C, the temperature at the top layers of PCM only system is still higher than 82°C meaning that no solidification happens in that area.

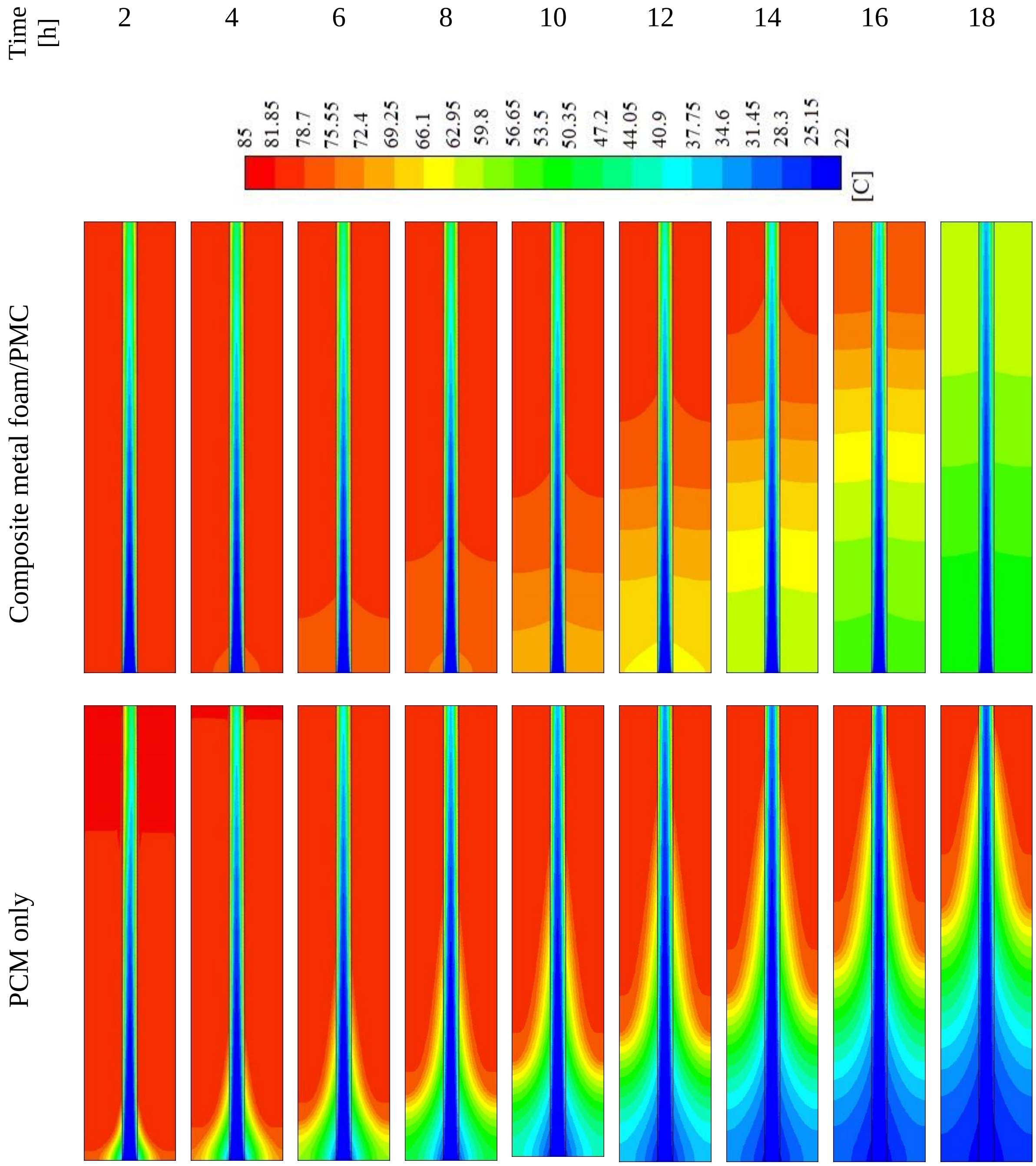

Fig. 5. The contours of temperature for the LHSHE with the composite PCM compared with the PCM only at different times for the inlet air temperature of 22°C

Figs. 6-a and 6-b display the variation of PCM temperature at different points at the middle of PCM shell at different heights for the LHSHE with the composite PCM and the PCM only, respectively. In the temperature profile, three different scenarios happened. The initial drop in temperature is due to the temperature difference from the initial temperature (85°C) to the liquidus temperature (82°C). In the mushy zone, the PCM solidifies and the temperature drops down from the liquidus temperature (82°C) to the solidus temperature (77°C) as increasingly higher proportion becomes solid. Then, the temperature decreases in solid phase until the PCM reaches the same temperature as the air. Note that in this study, the simulation is terminated when all the PCM solidifies and the latent stored heat is gained by the air. As shown, for the composite case, due to the presence of high conductivity metal foam and as a result higher heat transfer rate from top to the bottom layers, the temperatures of different points are closer to each other compared with the PCM only system.

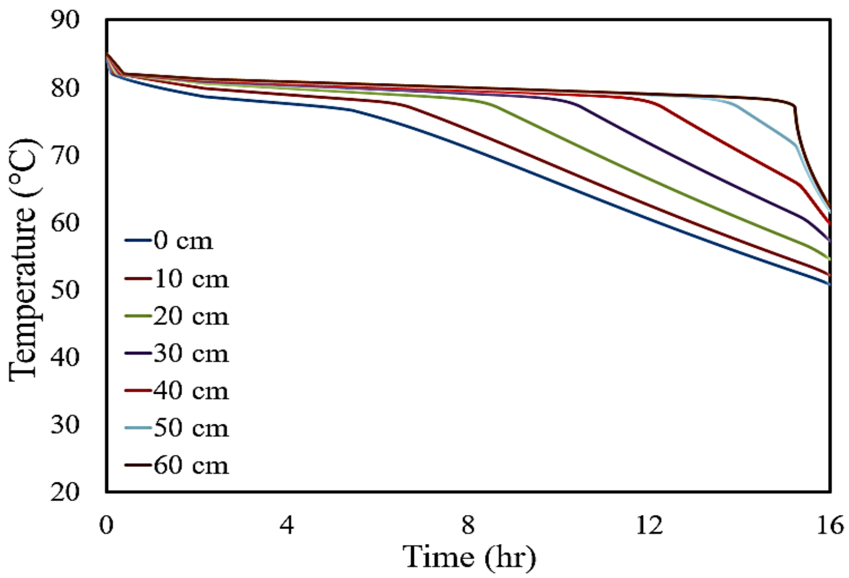

a

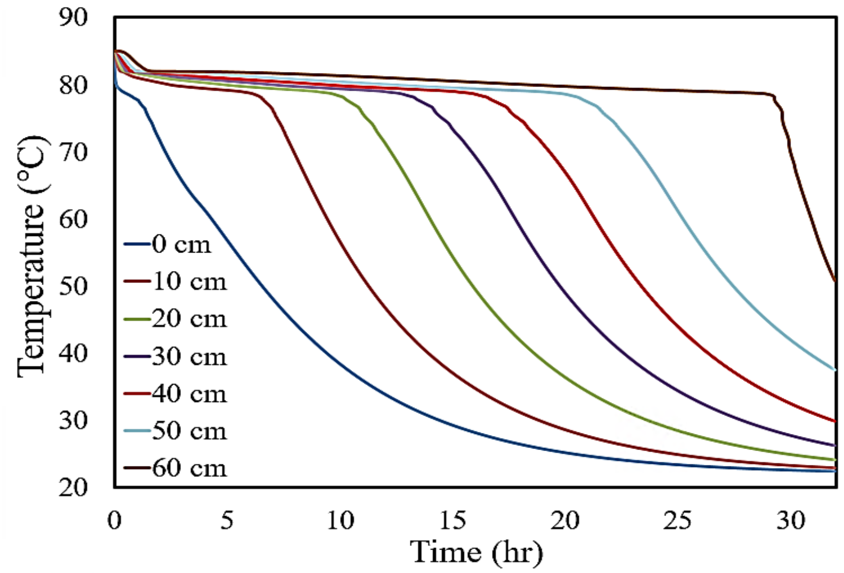

b

Fig. 6. The variation of PCM temperature at different locations of the LHSHE with the a) composite PCM and b) PCM only for the inlet air temperature of 22°C

Fig. 7 displays the mean temperature of PCM and air of the LHSHE with both composite PCM and PCM only. With the elapse of time, the average temperatures of PCM decreases due to transferring heat from the PCM to the air. Since the PCM loses its heat and as a result its temperature drops, the average temperature of the air also decreases. Furthermore, the PCM and air mean temperatures for the composite PCM is higher than that for the PCM only case shows the advantageous effect of the porous media in the LHSHE. The reason is due to the effect of the porous medium and as a result higher rate of conduction heat transfer in the composite PCM than the convection heat transfer in the PCM only. In the composite case, the heat can be transferred to the air faster by the porous medium and the heat exchanger can use a higher capacity of the latent heat from the composite case which can maintain a more uniform temperature distribution in the domain compared to the PCM only.

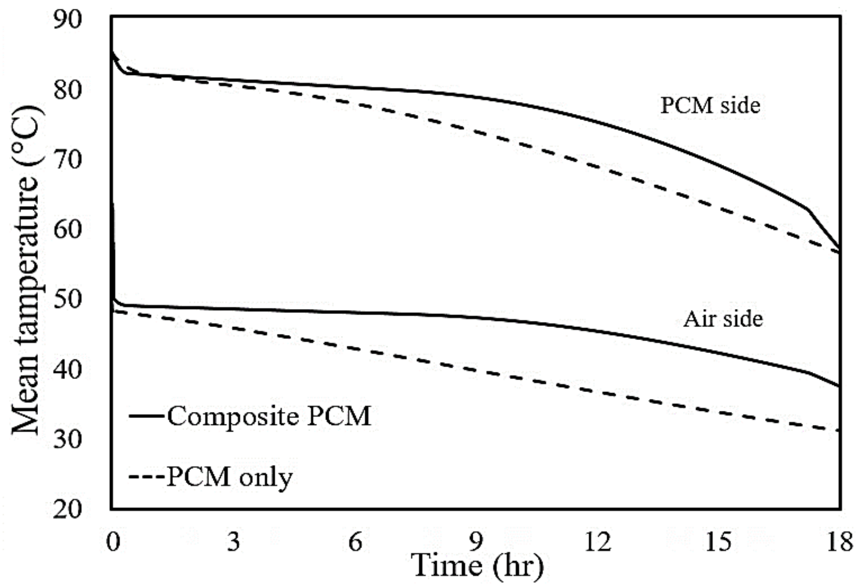

Fig. 7. The variation of PCM and air mean temperatures for the LHS system with the composite PCM compared with the PCM only for the inlet air temperature of 22°C

Fig. 8 displays the contour plots of the PCM liquid fraction for the systems with and without the metal foam at different times. The LHSHE with a composite PCM releases more heat to the air and therefore solidifies in less time across the entire domain. In the initial hours, in the LHSHE with the composite PCM, heat is transferred more by the metal foam than the PCM and therefore, the liquid fraction is less than that for the PCM only system. After that, when the entire domain becomes colder, a larger proportion of PCM solidifies and more heat is released to the air channel with the composite PCM-air system. For the PCM only case, natural convection is dominant and in the liquid zone, the gravity generates a big circulation in the domain where downward flow occurred near the air channel with a higher magnitude of velocity and then moves upward near the insulated wall of PCM container.

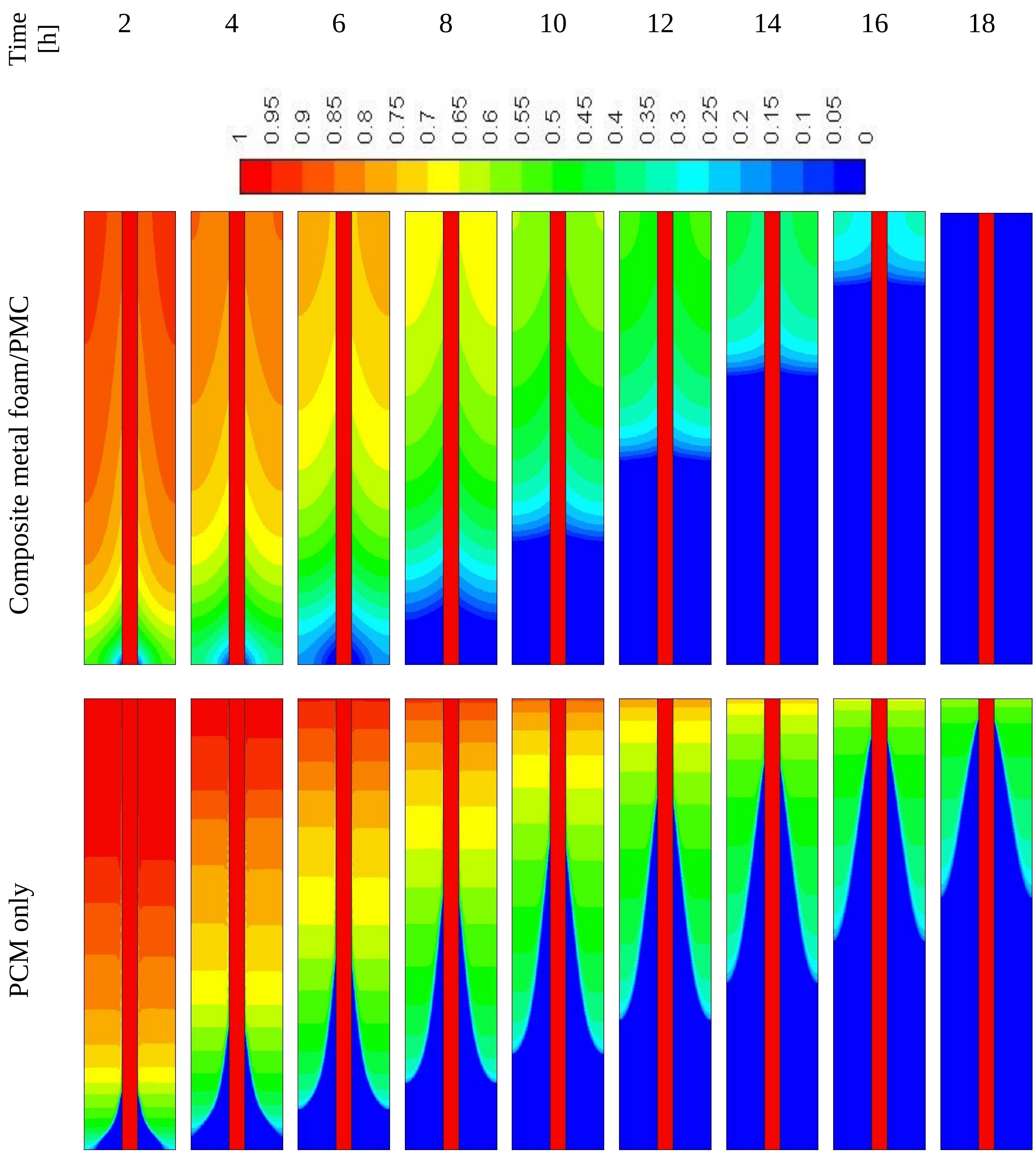

Fig. 8. The contours of the liquid fraction for the LHSHE with the composite PCM compared with the PCM only system at different times for the inlet air temperature of 22°C

Fig. 9 illustrates the variation of the PCM liquid fraction as a function of time for the LHSHE with and without the metal foam. After almost 17.25 hours, for the composite PCM-air heat exchanger, all the latent heat releases from the PCM and the liquid fraction of PCM reaches to zero. However, at this time, the liquid fraction of the PCM only-air heat exchanger is almost 0.13 and 13% of the total latent heat is not released from the PCM to the air, remaining as latent heat in the system at this time. Moreover, the total solidification time is almost 31 hours for the PCM only-air heat exchanger.

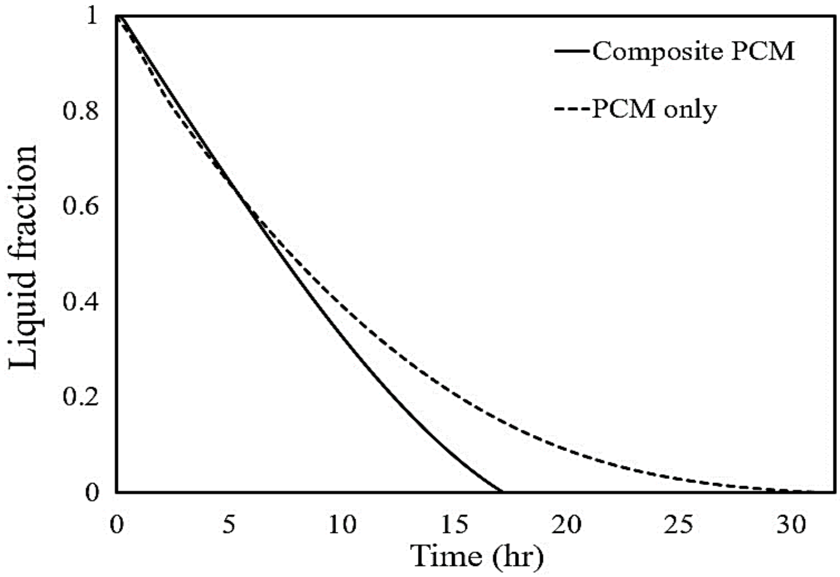

Fig. 9. The variation of liquid fraction of the LHSHE with the composite PCM compared with the PCM only at different times for the inlet air temperature of 22°C

Fig. 10 illustrates the variation of mean air-temperature difference of the system. The temperature difference for the composite LHSHE is much higher than that for the PCM only system. The mean air-temperature difference is almost 38°C at the beginning of heat retrieval and then reaches 26.8° for the composite system and 21.6°C for the PCM only system at 17.25 hours, when the PCM solidifies in the composite case. The composite system at that time can generate a higher mean temperature difference by almost 24% higher than the PCM only system. Furthermore, the mean temperature difference is almost constant for the first 8 hours and then reduces by almost 11°C in the composite PCM case; however, for the PCM only, the mean temperature difference always drops down at a constant rate. For the first 12 hours, for the composite system, the mean temperature deference decreases from almost 36°C to 32°C which means almost 4°C reduction in the temperature. However, for the PCM only system, almost 18°C reduction in the mean temperature difference occurs in the outlet air temperature

Note that due to the laminar flow of the air in the channel and hence heating the air in contact with the heat exchanger surface and relying on thermal conduction to heat the air in the centre of the channel, there is a temperature profile across the outlet air and the average value of the temperature at the outlet (T_{out}) is considered in Fig. 10.

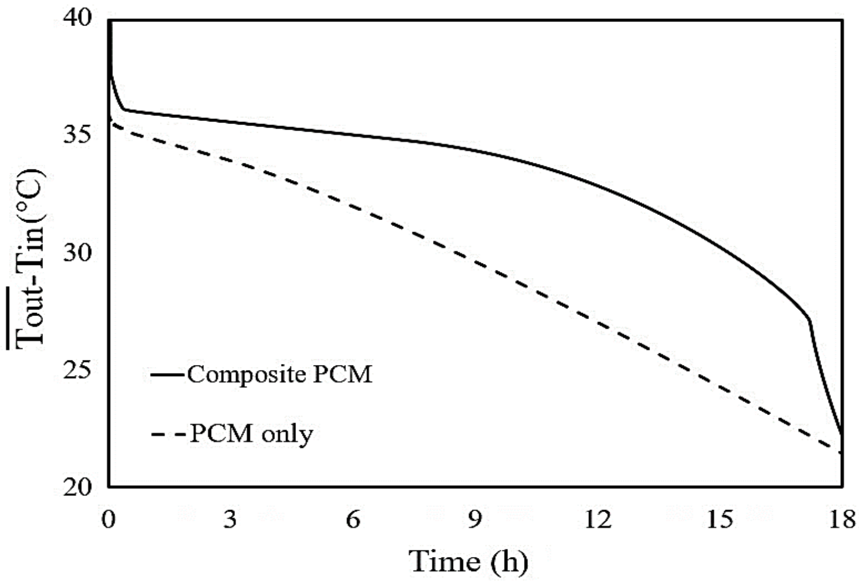

Fig. 10. The variation of mean air temperature difference as a function of time for the composite PCM LHSHE compared with the PCM only case for the inlet air temperature of 22°C

Table 2 presents the solidification time, the heat storage capacity, rate, density and rate density of the heat retrieval unit with and without the metal foam. Note that the negative numbers in Table 2 is due to heat retrieval from the system in the solidification process. The solidification time improves by almost 45% by using the composite PCM unit compared with the PCM only system. Due to the porosity of 95%, the total heat capacity of the composite PCM system is 5% less than that for the PCM only case; however, the rate of heat retrieval for the composite PCM case is almost 73% higher than the PCM only system due to the much lower solidification time. Furthermore, since 5% of the composite PCM case includes copper which is heavy, the heat retrieval density of PCM only system which is equal to the latent heat of fusion is 36% higher than the composite system. To consider both effect of solidification time and mass, the heat retrieval density of the composite PCM is 16% higher than that for the PCM only system. Therefore, the composite PCM unit also shows a higher performance than the PCM only system based on effective power rating analysis. It should be noted that since Table 2 is related to the solidification process when the heat releases from the PCM to the air, the values of Q, p, q and w are negative.

Table 2

The solidification time and power rating parameters for the composite PCM system compared with the PCM only system for the inlet air temperature of 22°C

Case	Solidification time (h)	Q (MJ)	p (W)	q (kJ/kg)	w (W/kg)
PCM only	31.51	-8.41	-74.18	-170	-1.5
Composite PCM	17.25	-7.99	-128.75	-108.2	-1.74

After turning on the heater when the room temperature reaches to a thermal equilibrium condition, an important issue is that the air-cooled heater is capable of maintaining the outlet temperature at an almost constant temperature. For the PCM-air heat exchanger, during the solidification process, it is important to maintain the outlet temperature of the heat transfer fluid at an almost constant temperature which is achieved by employing the foam inside the PCM container. Therefore, different inlet temperature of the air are also studied. By decreasing the inlet air temperature for both cases, the liquid fraction reduces at an almost constant rate. Table 3 lists the total solidification time. For the composite case, the total solidification time is almost 48% less than a system with the PCM only and the reduction rate decreases by increasing the inlet temperature of the air.

Table 3

The solidification time of LHSHE using composite PCM compared with PCM only for different inlet air temperatures

Inlet air temperature	PCM only	Composite PCM	Rate of reduction in solidification time, %
	Solidification time		
0°C	24.30	12.26	49.57
10°C	27.51	14.27	48.11
22°C	31.51	17.25	45.27

Table 4 shows the average air temperature at the outlet of the channel for different time periods for different inlet air temperatures. The outlet air temperature reduction with the lapse of time for the composite case is less than that with PCM only. For example, after 12 hours, for the inlet temperature of 0°C, the mean air temperature reduces by 10.9°C for the composite PCM system while it is 15.9°C for the PCM only system. Furthermore, by decreasing the temperature of inlet air, the reduction in the outlet air temperature increases.

Table 4

Mean outlet temperature of air at different time periods for different inlet air temperatures for different inlet air temperatures

Inlet air temperature	0-2 hr		2-4 hr		4-6 hr		6-8 hr		8-10 hr		10-12 hr	
	PCM only	composite	PCM only	composite	PCM only	composite	PCM only	composite	PCM only	composite	PCM only	composite
0°C	**47.5**	**50.3**	43.3	47.1	40.5	46.5	37.5	45.3	34.5	42.9	**31.6**	**39.4**
10°C	**51.1**	**53.7**	48.9	51.3	46.9	50.9	44.7	50.2	42.5	49.0	**40.2**	**47.1**
22°C	**57.4**	**58.2**	56.0	57.6	54.7	57.3	53.2	56.9	51.6	56.4	**49.9**	**55.5**

The effect of inlet air temperature is shown in Figs. 11-a and 11-b. For the composite PCM case, for the first 10 hours, the temperature difference variation is much lower than the PCM only case which shows the significant advantage of LHSHE with the composite PCM.

Furthermore, as expected, the mean outlet temperature increases for a lower inlet air temperature during the lowest solidification time.

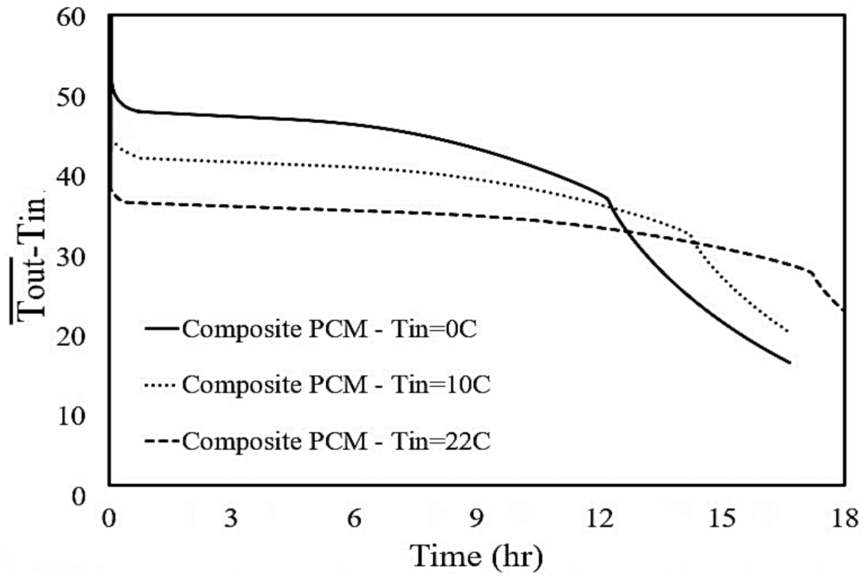

a)

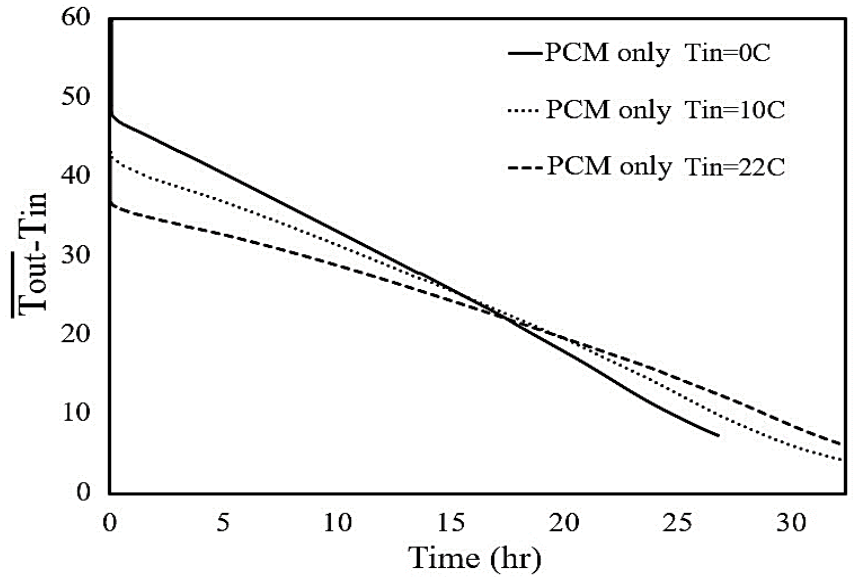

b)

Fig. 11. The variation of air temperature difference for different inlet air temperature for LHSHE with the a) composite PCM and b) PCM only for different inlet air temperatures

The solidification time and heat storage rate density for different inlet air temperatures are presented in Table 5. The advantage of the presence of copper foam can be seen based on both solidification time and rate density of heat retrieval. Furthermore, by reducing the inlet temperature of the air, the LHSHE rate density enhances due to a higher temperature difference between the PCM and the air results in a higher rate of heat retrieval in a shorter solidification time.

Table 5

The solidification time and rate density of heat retrieval for the composite PCM system compared with the PCM only system for difference inlet air temperatures for different inlet air temperatures

Inlet air temperature	Solidification time (h)		*w* (W/kg)	
	PCM only	Composite PCM	PCM only	Composite PCM
0°C	24.3	12.26	-1.94	-2.45
10°C	27.51	14.27	-1.72	-2.11
22°C	31.51	17.25	-1.5	-1.74

After evaluating the performance of composite PCM to air heat exchanger, it should be noted that the system should be studied from the cost point of view to demonstrate the value of using metal foam-PCM in domestic heaters. The cost of metal foams are expensive. PCMs are also still expensive. For example, a copper foam with the dimension of 20 mm×500 mm × 1000 mm is almost 405$ and the price of 1 kg PCM is almost 15$. Therefore, for the proposed dimension of the heater in this study, the total price of the copper foam and PCM is 3172$ which is expensive; however, it should be noted that this price is for lab scale and for a commercial product, the price is divided by 5 or 10 which makes it meaningful. Note that the price of available energy storage heaters with the same storage capacity using different sensible heat storage technique (magnetite storage cells) is around 800$. Furthermore, due to the technology of producing metal foams, the price of them is expensive now and hopefully in the future, it should be considerably less expensive than current prices. Moreover, instead of using metal foams, other high conductivity materials such as graphite can be used in order to provide a less expensive product. In this study, copper foam is utilized as an available high conductivity porous medium to show the potential of this product in providing a uniform output temperature for the heater.

7.2. 3-D simulation of the composite PCM-air heat exchanger compared with the case of PCM only

Due to a large number of computational nodes in 3-D simulations compared with 2-D cases, in practice, it is not feasible to simulate especially over long physical times [46]. Therefore, researchers have always tried to simplify the problem in order to consider it 2-D or even 1-D. In addition to the simplification, the way of heat transfer and boundary conditions of the problem affects the results [47].

In the present study, due to considering insulated boundaries for the PCM shell, it is expected that the results of 2-D and 3-D simulations are almost the same considering same governing equations. Figs. 12–a and 12-b illustrate the variation of the liquid fraction and outlet air temperature in different times for the 2-D and 3-D cases using equilibrium thermal model for the inlet air temperature of 22°C. The results of 2-D and 3-D simulations are almost the same. A little difference is related to the insulated boundaries at the walls of the heat exchanger. The velocity profile at the outlet of the air channel is also affected by the boundaries which makes a little more difference in the temperature difference of the air channel (see Fig. 12-b).

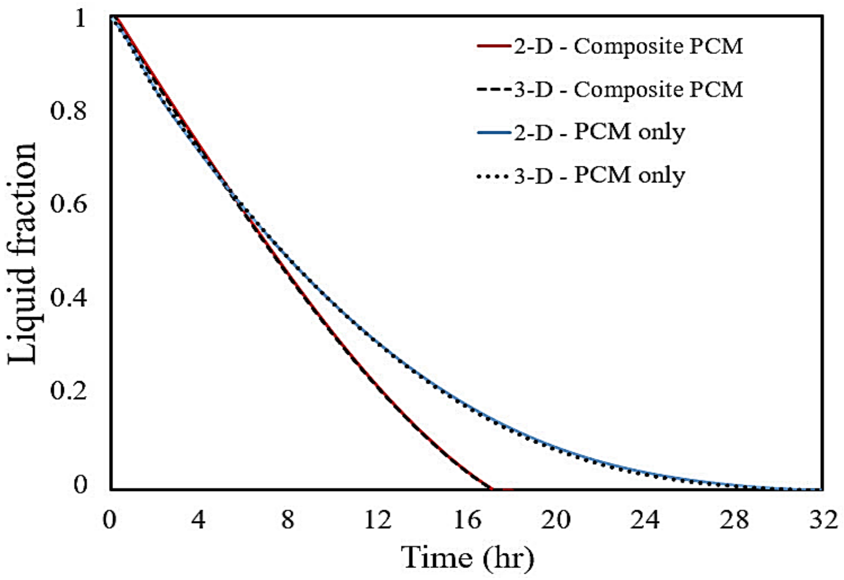

a)

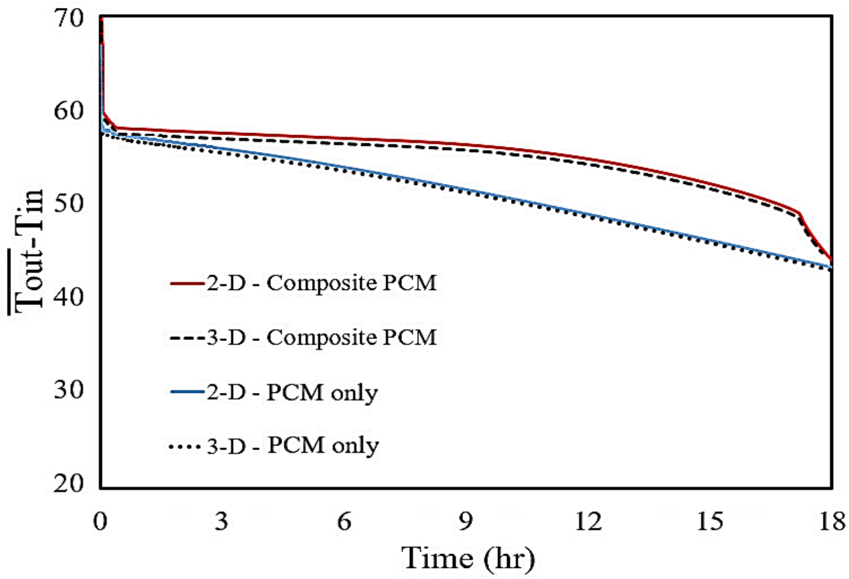

b)

Fig. 12. The comparison of a) the liquid fraction and b) the temperature difference at the air channel for the 2-D and 3-D simulations of LHSHE using the composite PCM and PCM only for the inlet air temperature of 22ºC

To better show the effect of metal foam, Fig. 13 displays the contour plot of the liquid fraction for the LHSHE with the PCM only (on the left) and the composite PCM (on the right) after 12 hours at three different horizontal sections in the domain for the inlet air temperature of 22°C. For the composite PCM, due to the effect of metal foam and enhancement of heat transfer in the domain, a uniform PCM liquid fraction the PCM liquid fraction can be seen in different sections. As shown in the middle section, all the PCM is in the mushy zone for the composite PCM with the liquid fraction of 0.2 due to the presence of a porous medium while for the PCM only, a narrow layer near the air channel solidifies completely and the liquid fraction for the other area is almost 0.5. So, it solidifies more slowly.

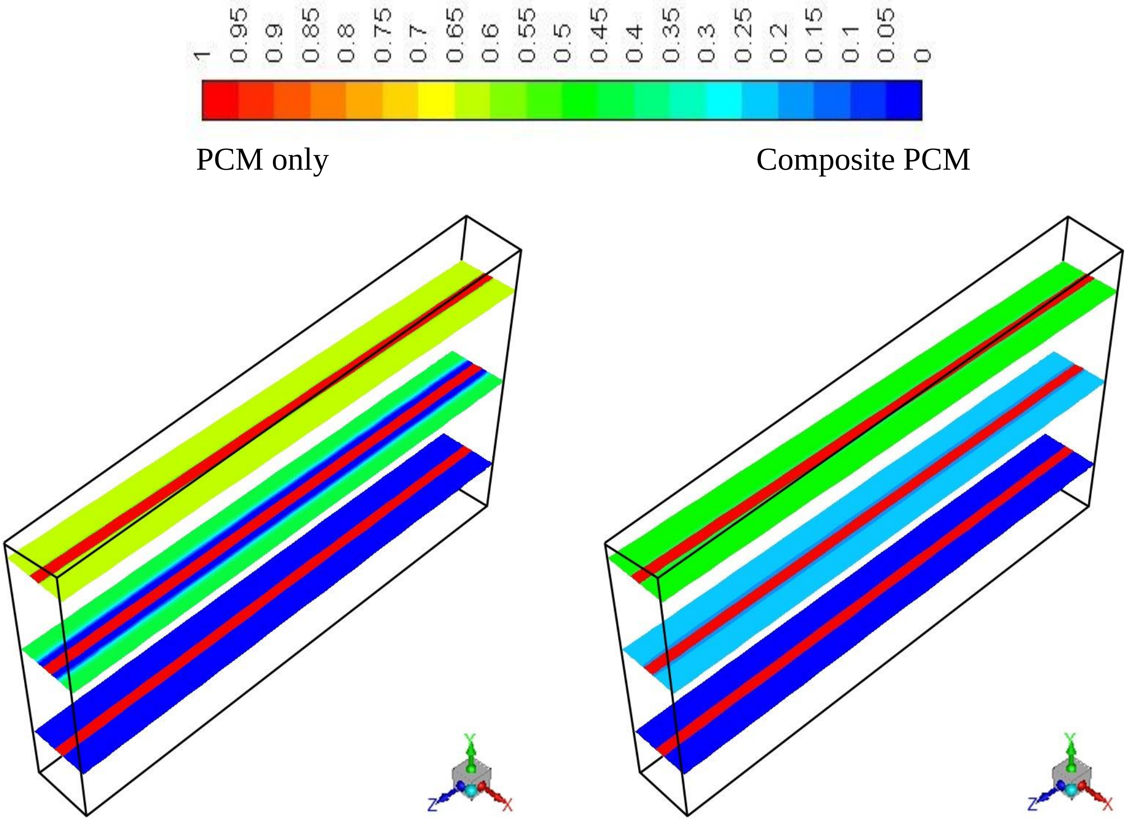

Fig. 13. The contour plot of liquid fraction at three different sections of the LHSHE with a composite metal foam/PCM compared with a PCM only for the inlet air temperature of 22ºC

Two thermal models including equilibrium and non-equilibrium can be used while the non-equilibrium model provides more accurate results due to considering heat transfer between the porous medium and the PCM [28, 41]. Fig. 14 shows the contour plot of the temperature distribution at the middle cross section of the LHSHE with the composite PCM using non-equilibrium thermal model for the inlet air temperature of 22°C. In the non-equilibrium thermal modelling of the LHSHE, a lower temperature difference can be seen in the domain and the temperature of different areas are closer to each other compared with the equilibrium thermal model shown in Fig. 5. It is noteworthy that, the non-equilibrium model cannot be used regularly in the 2-D case, due to generated porous boundaries at the walls between the air and the PCM and the limitation of coupled boundary condition for it in FLUENT software. Therefore, the non-equilibrium thermal modelling of the system is performed in 3-D simulations only.

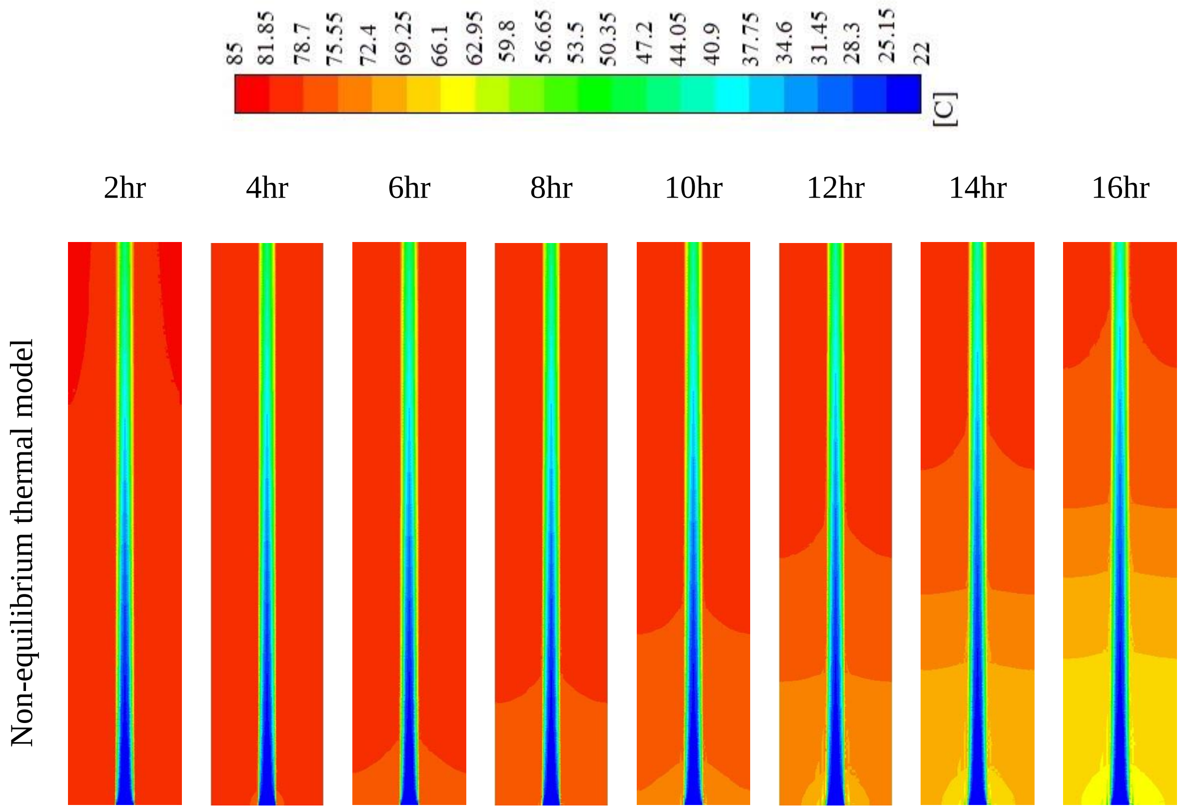

Fig. 14. The contour plot of temperature for the mid-section of the LHSHE with the composite PCM using non-equilibrium thermal model for the inlet air temperature of 22ºC

Fig. 15 displays the variation of the liquid fraction for the LHSHE with composite PCM using non-equilibrium thermal model compared with equilibrium one. The non-equilibrium model can predict the PCM liquid fraction more accurate and therefore a little difference is observed between the predicted results compared to equilibrium model. Since the simulated average temperature is higher for the non-equilibrium model, the liquid fraction is higher at the same time compared with the equilibrium one. The solidification time of the PCM using non-equilibrium model is 20% faster than that using equilibrium model.

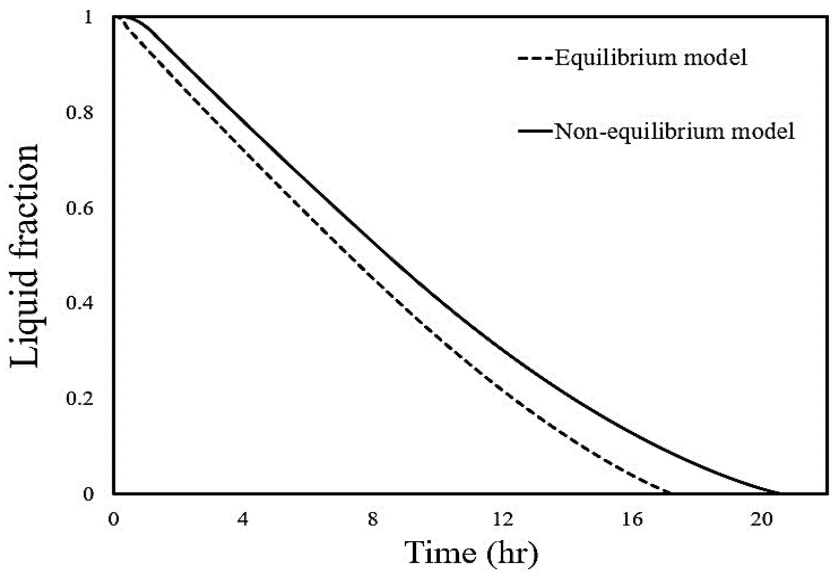

Fig. 15. The variation of liquid fraction for a 3-D LHSHE with a composite PCM using non-equilibrium thermal modelling compared with equilibrium one for the inlet air temperature of 22ºC

Fig. 16 illustrates the variation of the average temperature difference between the air channel outlet and inlet for the LHSHE with the composite PCM using non-equilibrium thermal model compared with equilibrium model. As shown, the average air temperature differences for the non-equilibrium model are close to the equilibrium model until half of the solidification process. Then, it is higher for the non-equilibrium model compared with the equilibrium model which shows more benefits of composite PCM-air heat exchanger than a PCM only-air system. Furthermore, this more physically representative simulation shows a lower variation in the outlet air temperature which is also another advantage for the purpose of space heating.

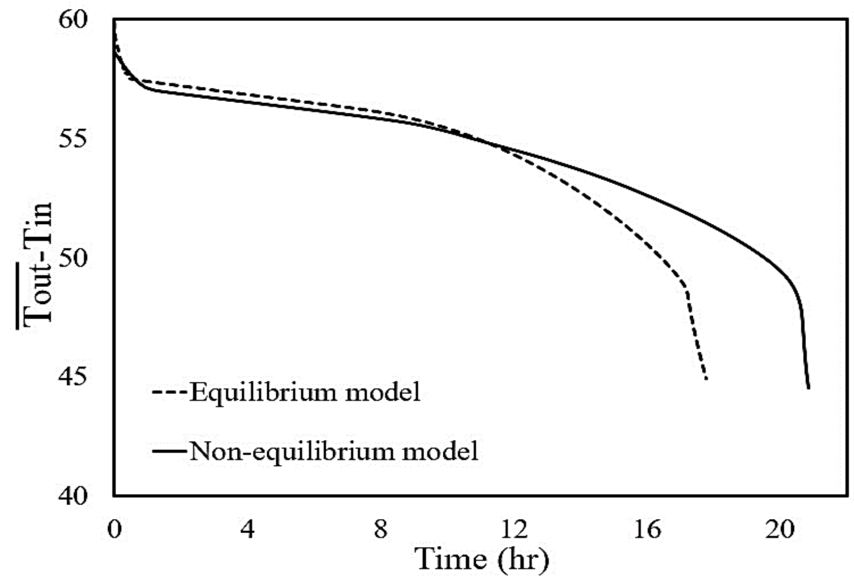

Fig. 16. The variation of temperature difference at the inlet and outlet of the air channel for a 3-D LHSHE with a composite PCM using non-equilibrium thermal modelling compared with equilibrium one for the inlet air temperature of 22ºC

8. Conclusion

A composite PCM-air heat exchanger was analysed in the solidification process. The results showed that a higher output air temperature with a lower reduction is occurred for the composite PCM-air heat exchanger compared with the PCM only-air system with the elapse of time. The reduction of almost 45% in the solidification time and 73% enhancement in the heat retrieval rate are achieved using composite copper foam PCM compared with PCM only case for the inlet air temperature of 22°C. After the solidification of the PCM, the mean outlet air temperature of LHSHE with a composite metal foam/PCM is almost 39°C after 17.25 hours for the inlet air temperature 22°C while it is almost 29°C after 31.5 hours for the system with the PCM only. After 12 hours, for the composite metal foam/PCM system, the mean air temperature reduces by almost 4°C while it is almost 18°C for the PCM only case. In the non-equilibrium modelling of the porous medium, a higher solidification time is achieved; however, a higher mean temperature of the outlet air with a lower reduction at the end of solidification process is obtained compared with the equilibrium model.

It can be concluded that this work has proved the application of composite metal foam/PCM LHSHE systems for domestic usage with regards to the performance of a PCM based heaters. In addition to providing a uniform output temperature which is essential for space heating, the system provides the required solidification time with a higher rate of heat retrieval to the air. The system also shows a significant performance in different room temperatures to provide a comfort thermal condition inside the building.

9. Acknowledgement

This work was funded by the EPSRC (Engineering and Physical Sciences Research Council) via Supergen Energy Storage II, grant reference EP/P003435/1, titled 'nano-Structured PCM Composites for Compact Space Heating: n-CoSH'.

Appendix A

Different number of cells are examined for both 2-D and 3-D cases to study the effect of grid sizes on the results. Note that due to the existence of natural convection in the y-direction, a higher number of nodes is applied in the y-direction. Figs. 17-a and 17-b illustrate the effect of cell number on the liquid fraction of PCM and mean outlet temperature of the air in the 2-D case of LHSHE with a composite metal foam/PCM, respectively. As shown, for the cell numbers of 57000 and 76000, the results are coincident. Therefore, the cell number of 57000 is chosen for the final mesh in the 2-D case.

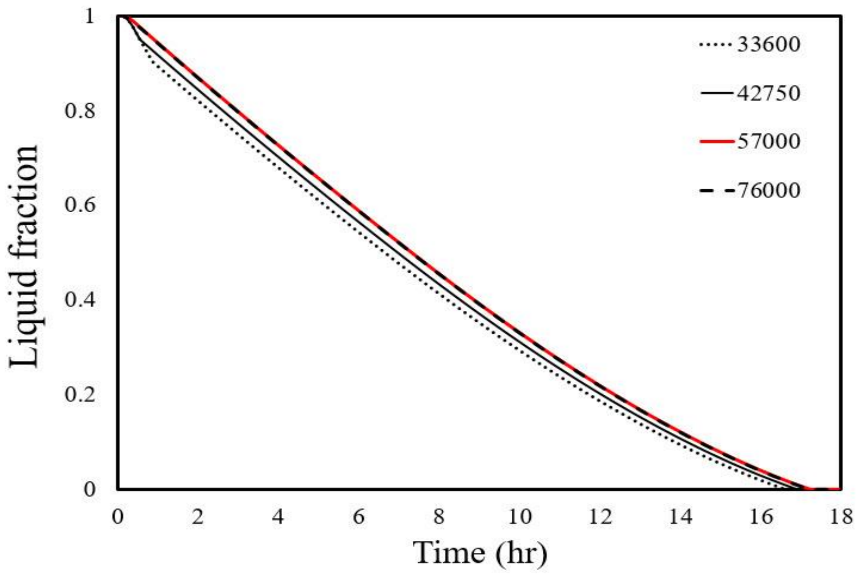

a)

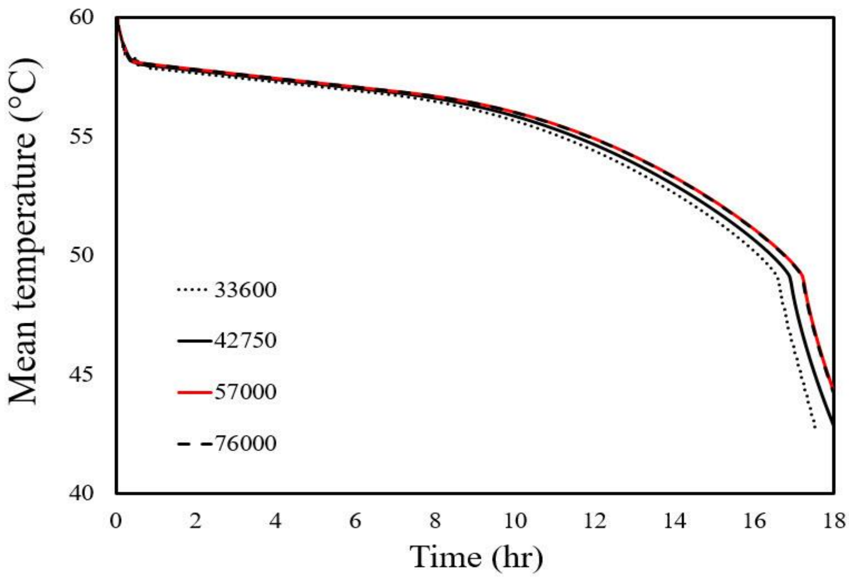

b)

Fig. 17. Effect of cell number on the a) liquid fraction of PCM and b) mean outlet temperature of the air in the 2-D case for the inlet air temperature of 22°C

Figs. 18-a and 18-b illustrate the effect of cell number on the liquid fraction of PCM and mean outlet temperature of the air in the 3-D case, respectively. The results are similar for the different grids; however, for the cell numbers of 380000 and 570000, the results are completely the same. Therefore, the cell number of 380000 is chosen for the final mesh in the 3-D simulations.

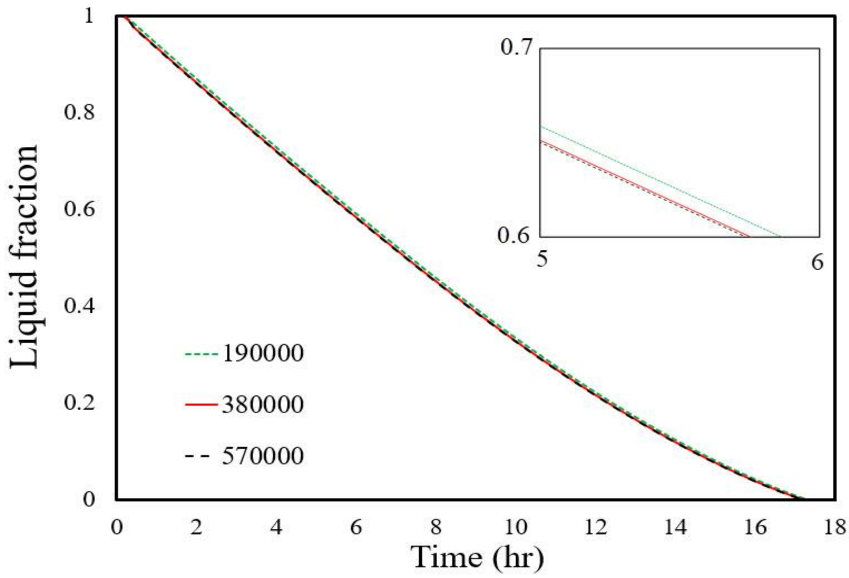

a)

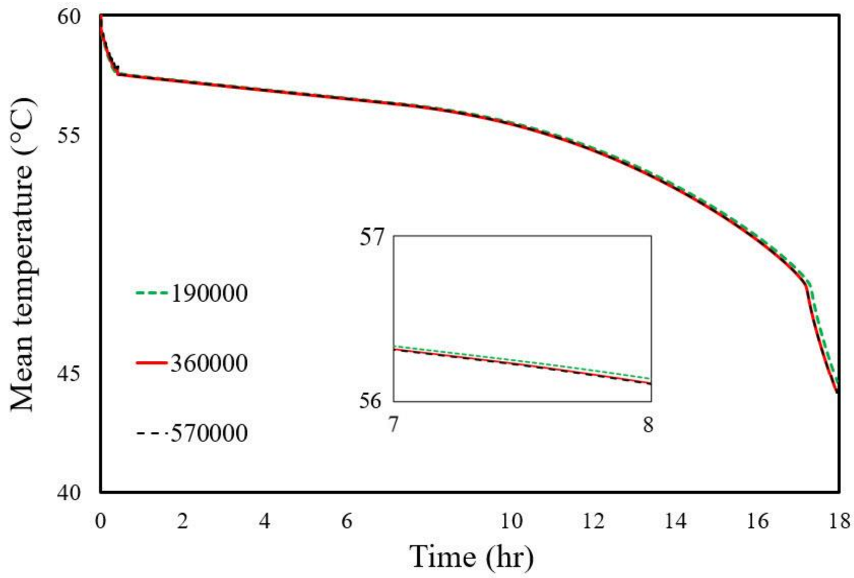

b)

Fig. 18. Effect of cell number on the a) liquid fraction of PCM and b) average outlet temperature of the air in the 3-D case for the inlet air temperature of 22°C

References

[1] Energy Consumption in the UK, Department of Business, Energy, and Industrial Strategy (BIES), July 2017.

[2] 2016 UK GREENHOUSE GAS EMISSIONS, PROVISIONAL FIGURES, Department for Business, Energy & Industrial Strategy (BEIS), March 2017.

[3] Z. Khan, Z. Khan, A. Ghafoor, A review of performance enhancement of PCM based latent heat storage system within the context of materials, thermal stability and compatibility, Energy Conversion and Management 115 (2016) 132-158.

[4] M. Aneke, M. Wang, Energy storage technologies and real life applications – A state of the art review, Applied Energy 179 (2016) 350-377.

[5] A.R. Shaibani, M.M. Keshtkar, P.T. Sardari, Thermo-economic analysis of a cold storage system in full and partial modes with two different scenarios: A case study, Journal of Energy Storage 24 (2019) 100783.

[6] J. Pereira da Cunha, P. Eames, Thermal energy storage for low and medium temperature applications using phase change materials – A review, Applied Energy 177 (2016) 227-238.

[7] M. Esapour, M.J. Hosseini, A.A. Ranjbar, Y. Pahamli, R. Bahrampoury, Phase change in multi-tube heat exchangers, Renewable Energy 85 (2016) 1017-1025.

[8] M. Delgado, A. Lázaro, J. Mazo, B. Zalba, Review on phase change material emulsions and microencapsulated phase change material slurries: Materials, heat transfer studies and applications, Renewable and Sustainable Energy Reviews 16(1) (2012) 253-273.

[9] A. Jamekhorshid, S.M. Sadrameli, M. Farid, A review of microencapsulation methods of phase change materials (PCMs) as a thermal energy storage (TES) medium, Renewable and Sustainable Energy Reviews 31 (2014) 531-542.

[10] B.R. Sushobhan, S.P. Kar, Thermal Modeling of Melting of Nano based Phase Change Material for Improvement of Thermal Energy Storage, Energy Procedia 109 (2017) 385-392.

[11] T. Oya, T. Nomura, N. Okinaka, T. Akiyama, Phase change composite based on porous nickel and erythritol, Applied Thermal Engineering 40 (2012) 373-377.

[12] T. Nomura, N. Okinaka, T. Akiyama, Impregnation of porous material with phase change material for thermal energy storage, Materials Chemistry and Physics 115(2) (2009) 846-850.

[13] A. Sarı, A. Karaipekli, Thermal conductivity and latent heat thermal energy storage characteristics of paraffin/expanded graphite composite as phase change material, Applied Thermal Engineering 27(8) (2007) 1271-1277.

[14] M. Esapour, M.J. Hosseini, A.A. Ranjbar, R. Bahrampoury, Numerical study on geometrical specifications and operational parameters of multi-tube heat storage systems, Applied Thermal Engineering 109 (2016) 351-363.

[15] M. Esapour, A. Hamzehnezhad, A.A. Rabienataj Darzi, M. Jourabian, Melting and solidification of PCM embedded in porous metal foam in horizontal multi-tube heat storage system, Energy Conversion and Management 171 (2018) 398-410.

[16] A. Shahsavar, A. Shaham, P. Talebizadehsardari, Wavy channels triple-tube LHS unit with sinusoidal variable wavelength in charging/discharging mechanism, International Communications in Heat and Mass Transfer 107 (2019) 93-105.

[17] B.V.S. Dinesh, A. Bhattacharya, Effect of foam geometry on heat absorption characteristics of PCM-metal foam composite thermal energy storage systems, International Journal of Heat and Mass Transfer 134 (2019) 866-883.

[18] M. Sheikholeslami, O. Mahian, Enhancement of PCM solidification using inorganic nanoparticles and an external magnetic field with application in energy storage systems, Journal of cleaner production 215 (2019) 963-977.

[19] A. Arshad, M. Jabbal, Y. Yan, J. Darkwa, The micro-/nano-PCMs for thermal energy storage systems: A state of art review, International Journal of Energy Research 43(11) (2019) 5572-5620.

[20] H.M. Ali, M.J. Ashraf, A. Giovannelli, M. Irfan, T.B. Irshad, H.M. Hamid, F. Hassan, A. Arshad, Thermal management of electronics: An experimental analysis of triangular, rectangular and circular pin-fin heat sinks for various PCMs, International Journal of Heat and Mass Transfer 123 (2018) 272-284.

[21] H.M. Ali, A. Arshad, M. Jabbal, P.G. Verdin, Thermal management of electronics devices with PCMs filled pin-fin heat sinks: A comparison, International Journal of Heat and Mass Transfer 117 (2018) 1199-1204.

[22] Z.X. Li, A.A.A.A. Al-Rashed, M. Rostamzadeh, R. Kalbasi, A. Shahsavar, M. Afrand, Heat transfer reduction in buildings by embedding phase change material in multi-layer walls: Effects of repositioning, thermophysical properties and thickness of PCM, Energy Conversion and Management 195 (2019) 43-56.

[23] P. Talebizadeh Sardari, G.S. Walker, M. Gillott, D. Grant, D. Giddings, Numerical modelling of phase change material melting process embedded in porous media: Effect of heat storage size, Proceedings of the Institution of Mechanical Engineers, Part A: Journal of Power and Energy (2019) 0957650919862974.

[24] H.I. Mohammed, P.T. Sardari, D. Giddings, Multiphase flow and boiling heat transfer modelling of nanofluids in horizontal tubes embedded in a metal foam, International Journal of Thermal Sciences 146 (2019) 106099.

[25] O. Mesalhy, K. Lafdi, A. Elgafy, K. Bowman, Numerical study for enhancing the thermal conductivity of phase change material (PCM) storage using high thermal conductivity porous matrix, Energy Conversion and Management 46(6) (2005) 847-867.

[26] C.Y. Zhao, W. Lu, Y. Tian, Heat transfer enhancement for thermal energy storage using metal foams embedded within phase change materials (PCMs), Solar Energy 84(8) (2010) 1402-1412.

[27] Y. Tian, C.Y. Zhao, A numerical investigation of heat transfer in phase change materials (PCMs) embedded in porous metals, Energy 36(9) (2011) 5539-5546.

[28] Z. Liu, Y. Yao, H. Wu, Numerical modeling for solid–liquid phase change phenomena in porous media: Shell-and-tube type latent heat thermal energy storage, Applied Energy 112 (2013) 1222-1232.

[29] P. Zhang, Z.N. Meng, H. Zhu, Y.L. Wang, S.P. Peng, Melting heat transfer characteristics of a composite phase change material fabricated by paraffin and metal foam, Applied Energy 185 (2017) 1971-1983.

[30] X. Wang, J. Liu, Y. Zhang, H. Di, Y. Jiang, Experimental research on a kind of novel high temperature phase change storage heater, Energy conversion and management 47(15-16) (2006) 2211-2222.

[31] B. Dechesne, S. Gendebien, J. Martens, V. Lemort, Designing And Testing An Air-PCM Heat Exchanger For Building Ventilation Application Coupled To Energy Storage, 15th International Refrigeration and Air Conditioning Conference, Purdue,, July 14-17, 2014.

[32] E. Osterman, V. Butala, U. Stritih, PCM thermal storage system for 'free' heating and cooling of buildings, Energy and Buildings 106 (2015) 125-133.

[33] P. Wang, X. Wang, Y. Huang, C. Li, Z. Peng, Y. Ding, Thermal energy charging behaviour of a heat exchange device with a zigzag plate configuration containing multi-phase-change-materials (m-PCMs), Applied Energy 142 (2015) 328-336.

[34] S. Gendebien, J. Martens, L. Prieels, V. Lemort, Designing an air-to-air heat exchanger dedicated to single room ventilation with heat recovery, Building Simulation 11(1) (2018) 103-113.

[35] R.T. GmbH, RT82 data sheet.

[36] D.A. Nield, A. Bejan, Convection in Porous Media, Springer International Publishing2017.

[37] J.M. Mahdi, E.C. Nsofor, Melting enhancement in triplex-tube latent heat energy storage system using nanoparticles-metal foam combination, Applied Energy 191 (2017) 22-34.

[38] M. Moghimi, P. Talebizadeh, M. Mehrabian, Heat generation/absorption effects on magnetohydrodynamic natural convection flow over a sphere in a non-Darcian porous medium, Proceedings of the Institution of Mechanical Engineers, Part E: Journal of Process Mechanical Engineering 225(1) (2011) 29-39.

[39] A. Shahsavar, A.A.A.A. Al-Rashed, S. Entezari, P.T. Sardari, Melting and Solidification Characteristics of a Double-Pipe Latent Heat Storage System with Sinusoidal Wavy Channels Embedded in a Porous Medium, Energy (2019).

[40] A. Žukauskas, Heat Transfer from Tubes in Crossflow, in: J.P. Hartnett, T.F. Irvine (Eds.), Advances in Heat Transfer, Elsevier1972, pp. 93-160.

[41] P. Zhang, X. Xiao, Z.N. Meng, M. Li, Heat transfer characteristics of a molten-salt thermal energy storage unit with and without heat transfer enhancement, Applied Energy 137 (2015) 758-772.

[42] A.A. Al-abidi, S. Bin Mat, K. Sopian, M.Y. Sulaiman, A.T. Mohammed, CFD applications for latent heat thermal energy storage: a review, Renewable and Sustainable Energy Reviews 20 (2013) 353-363.

[43] Y. Xu, Q. Ren, Z.-J. Zheng, Y.-L. He, Evaluation and optimization of melting performance for a latent heat thermal energy storage unit partially filled with porous media, Applied energy 193 (2017) 84-95.

[44] ASHRAE STANDARDS SET, American Society of Heating, Refrigerating and Air-Conditioning Engineers (ASHRAE), 2013.

[45] V. Golkarfard, P. Talebizadeh, Numerical comparison of airborne particles deposition and dispersion in radiator and floor heating systems, Advanced Powder Technology 25(1) (2013) 389–397.

[46] A.J. Parry, P.C. Eames, F.B. Agyenim, Modeling of Thermal Energy Storage Shell-and-Tube Heat Exchanger, Heat Transfer Engineering 35(1) (2014) 1-14.

[47] M.J. Huang, P.C. Eames, B. Norton, Comparison of a small-scale 3D PCM thermal control model with a validated 2D PCM thermal control model, Solar Energy Materials and Solar Cells 90(13) (2006) 1961-1972.